

Flexible Dataset Distillation: Learn Labels Instead of Images

Ondrej Bohdal¹, Yongxin Yang¹, Timothy Hospedales¹

¹The University of Edinburgh

{ondrej.bohdal, yongxin.yang, t.hospedales}@ed.ac.uk

Abstract

We study the problem of dataset distillation – creating a small set of synthetic examples capable of training a good model. In particular, we study the problem of *label* distillation – creating synthetic labels for a small set of real images, and show it to be more effective than the prior *image*-based approach to dataset distillation. Methodologically, we introduce a more robust and flexible meta-learning algorithm for distillation, as well as an effective first-order strategy based on convex optimization layers. Distilling labels with our new algorithm leads to improved results over prior image-based distillation. More importantly, it leads to clear improvements in flexibility of the distilled dataset in terms of compatibility with off-the-shelf optimizers and diverse neural architectures. Interestingly, label distillation can also be applied across datasets, for example enabling learning Japanese character recognition by training only on synthetically labeled English letters.

1 Introduction

Distillation is a topical area of neural network research that initially began with the goal of extracting the knowledge of a large pre-trained model and compiling it into a smaller model, while retaining similar performance (Hinton, Vinyals, and Dean 2014). The notion of distillation has since found numerous applications and uses including the possibility of *dataset* distillation (Wang et al. 2018): extracting the knowledge of a large dataset and compiling it into a small set of carefully crafted examples, such that a model trained on the small dataset alone achieves good performance. This is of scientific interest as a tool to study neural network generalisation under small sample conditions. More practically, it has the potential to address the large and growing logistical and energy hurdle of neural network training, if adequate neural networks can be quickly trained on small distilled datasets rather than massive raw datasets.

Nevertheless, progress towards the vision of dataset distillation has been limited as the performance of existing methods (Wang et al. 2018; Sucholutsky and Schonlau 2019) trained from random initialization is far from that of full dataset supervised learning. More fundamentally, existing approaches are relatively *inflexible* in terms of the distilled data being over-fitted to the training conditions under which it was generated. While there is some robustness to choice of initialization weights (Wang et al. 2018), the distilled dataset

is largely specific to the architecture used to train it (thus preventing its use to accelerate neural architecture search – NAS, for example), and must use a highly-customized learner (a specific image visitation sequence, a specific sequence of carefully chosen meta-learned learning rates, and a specific number of learning steps). Altogether these constraints mean that existing distilled datasets are not general purpose enough to be useful in practice, e.g. with off-the-shelf learning algorithms. We propose a more *flexible* approach to dataset distillation underpinned by both algorithmic improvements and changes to the problem definition.

Rather than creating synthetic images (Wang et al. 2018) for arbitrary labels, or a combination of synthetic images and soft labels (Sucholutsky and Schonlau 2019), we focus on crafting synthetic labels for arbitrarily chosen standard images. Compared to these prior approaches focused on synthetic images, label distillation benefits from exploiting the data statistics of natural images and the lower-dimensionality of labels compared to images as parameters for meta-learning. Practically, this leads to improved performance compared to prior image distillation approaches. As a byproduct, this enables a new kind of cross-dataset knowledge distillation (Figure 1). One can learn solely on a source dataset (such as English characters) with synthetic distilled labels, and apply the learned model to recognise concepts in a disjoint target dataset (such as Japanese characters). Surprisingly, it turns out that models can make progress on learning to recognise Japanese only through exposure to English characters with synthetic labels.

Methodologically, we define a new meta-learning algorithm for distillation that does not require costly evaluation of multiple inner-loop (model-training) steps for each iteration of distillation. More importantly our algorithm leads to a more flexible distilled dataset that is better transferable across optimizers, architectures, learning iterations, etc. Furthermore, where existing dataset distillation algorithms rely on second-order gradients, we introduce an alternative learning strategy based on convex optimization layers that avoids high-order gradients and provides better optimization, thus improving the quality of the distilled dataset.

In summary, we contribute: (1) A dataset distillation method that produces flexible distilled datasets that exhibit transferability across learning algorithms. This brings us one step closer to producing useful general-purpose dis-

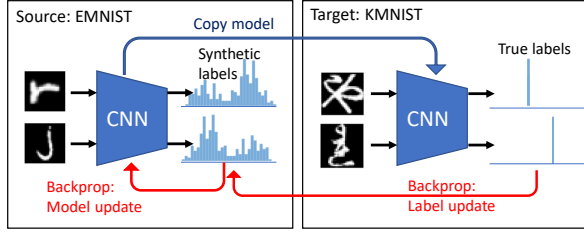


Figure 1: Label distillation enables training a model that can classify Japanese characters after being trained only on English letters and synthetic labels. Labels are updated only during meta-training, after which a new model is trained.

tilled datasets. (2) Our distilled datasets can be used to train higher performance models than those prior work. (3) We introduce the novel concept of cross-dataset distillation, and demonstrate proofs of concept for this curiosity, such as English→Japanese letter recognition.

2 Related Work

Dataset Distillation. Most closely related to our work is Dataset (Wang et al. 2018) and Soft-Label Dataset Distillation (Sucholutsky and Schonlau 2019). They focus on the problem of distilling a dataset or model (Micaelli and Storkey 2019) into a small number of example images, which are then used to train a new model. This can be seen as solving a meta-learning problem with respect to model’s training data (Hospedales et al. 2020). The common approach is to initialise the distilled dataset randomly, use the distilled data to train a model, and then backpropagate through the model and its training updates to take gradient steps on the dataset. Since the ‘inner’ model training algorithm is gradient-based, this leads to high-order gradients. To make this process tractable, the original Dataset Distillation (Wang et al. 2018) uses only a few gradient steps in its inner loop (as per other famous meta-learners (Finn, Abbeel, and Levine 2017)). To ensure that sufficient learning progress is made with few updates, it also meta-learns a fixed set of optimal learning rates to use at each step. This balances tractability and efficacy, but causes the distilled dataset to be ‘locked in’ to the customized optimizer rather than serve as a general purpose dataset, which also prevents its use for NAS (Shleifer and Prokop 2019). In this work we define an online meta-learning procedure that simultaneously learns the dataset and the base model. This enables us to tractably take more gradient steps, and ultimately to produce a performant yet flexible general purpose distilled dataset.

There are various motivations for dataset distillation, but the most practically intriguing is to summarize a dataset in compressed form to accelerate model training. In this sense it is related to fields such as dataset pruning (Angelova, Abu-Mostafa, and Perona 2005; Felzenszwalb et al. 2010), core-set construction (Tsang, Kwok, and Cheung 2005; Sener and Savarese 2018) and instance selection (Olvera-López et al. 2010) focusing on dataset summarization through a small number of examples. The key difference is summarization

methods *select* a relatively large part of the data (e.g. at least 10%), while distillation extends down to using 10 images per category ($\approx 0.2\%$ of CIFAR-10 data) through example *synthesis*. We retain original data (like summarization methods), but synthesize labels (like distillation). This leads to a surprising observation – it is possible to synthesize labels for a few fixed examples so a model trained on these examples can directly (without any fine-tuning) solve a different problem with a different label space (Figure 1).

Meta-Learning. Meta-learning algorithms can often be grouped (Hospedales et al. 2020) into offline approaches (e.g. Wang et al. (2018); Finn, Abbeel, and Levine (2017)) that solve an inner optimization at every iteration of an outer optimization; and online approaches that solve the base and meta-learning problem simultaneously (e.g. Balaji, Sankaranarayanan, and Chellappa (2018); Li et al. (2019)). Meta-learning is related to hyperparameter optimization, for example Maclaurin, Duvenaud, and Adams (2015); Lorraine, Vicol, and Duvenaud (2020) efficiently unroll through many steps of optimization like offline meta-learning, while Luketina et al. (2016) optimize hyperparameters and the base model like online meta-learning. Online approaches are typically faster, but optimize meta-parameters for a single problem. Offline approaches are slower and typically limit the length of the inner optimization for tractability, but can often find meta-parameters that solve a distribution of tasks (as different tasks are drawn in each outer-loop iteration). In dataset distillation, the notion of ‘distribution over tasks’ corresponds to finding a dataset that can successfully train a network in many settings, such as different initial conditions (Wang et al. 2018). Our distillation algorithm is a novel hybrid of these two families. We efficiently solve the base and meta-tasks simultaneously as per the online approaches, and are thus able to use more inner-loop steps. However, we also learn to solve many ‘tasks’ by detecting meta-overfitting and sampling a new ‘task’ when this occurs. This leads to an excellent combination of efficacy and efficiency.

Finally, most gradient-based meta-learning algorithms rely on costly and often unstable higher-order gradients (Hospedales et al. 2020; Finn, Abbeel, and Levine 2017; Wang et al. 2018), or else make simple shortest-path first-order approximations (Nichol, Achiam, and Schulman 2018). Instability and large variance of higher-order gradients may make meta-learning less effective (Liu, Socher, and Xiong 2019; Farquhar, Whiteson, and Foerster 2019), which motivates us to search for alternatives. We are inspired by recent approaches in few-shot learning (Bertinetto et al. 2019; Lee et al. 2019) that avoid this issue through the use of convex optimization layers. We introduce the notion of a pseudo-gradient that enables this idea to scale beyond the few-shot setting to general meta-learning problems such as dataset distillation.

3 Methods

We aim to meta-learn synthetic labels for a fixed set of *base* examples that can be used to train a randomly initialized

model. This corresponds to an objective such as (Eq. 1):

$$\tilde{\mathbf{y}}^* = \arg \min_{\tilde{\mathbf{y}}} \ell((\mathbf{x}_t, \mathbf{y}_t), \theta - \alpha \nabla_{\theta} \ell((\tilde{\mathbf{x}}, \tilde{\mathbf{y}}), \theta)), \quad (1)$$

where $\tilde{\mathbf{y}}$ are the distilled labels for base examples $\tilde{\mathbf{x}}$, $(\mathbf{x}_t, \mathbf{y}_t)$ are the target set examples and labels and θ is the neural network model learned with rate α and loss ℓ (we use cross-entropy). We learn soft labels, so the dimensionality of each label is the number of classes C to distill. One gradient step is shown above, but in general there may be multiple steps.

One option to achieve objective in (Eq. 1) would be to follow Wang et al. (2018) and simulate the whole training procedure for multiple gradient steps ∇_{θ} within the inner loop. However, this requires back-propagating through a long inner loop, and ultimately requires a fixed training schedule with optimized learning rates. We aim to produce a dataset that can be used in a standard training pipeline downstream (e.g. Adam optimizer with the default parameters).

Our first modification to the standard pipeline is to perform gradient descent iteratively on the model and the distilled labels, rather than performing many inner (model) steps for each outer (dataset) step. This increases efficiency significantly due to a shorter compute graph for backpropagation. Nevertheless, when there are very few training examples, the model converges quickly to an over-fitted local minimum, likely within a few hundred iterations. To manage this, our innovation is to detect overfitting when it occurs, reset the model to a new random initialization and keep training. Specifically, we measure the moving average of target problem accuracy, and when it has not improved for set number of iterations, we reset the model. This periodic reset of the model after varying number of iterations is helpful for learning labels that are useful for all stages of training and thus less sensitive to the number of iterations used. To ensure scalability to any number of examples, we sample a mini-batch of base examples and synthetic labels and use those to update the model, which also better aligns with standard training practice. Once label distillation is done, we train a new model from scratch using random initial weights, given the base examples and learned synthetic labels.

We propose and evaluate two label distillation algorithms: a second-order version that performs one update step within the inner loop; and a first-order version that uses a closed form solution of ridge regression to find optimal classifier weights for the base examples.

Vanilla Second-Order Version. The training procedure includes both inner and outer loop. The inner loop consists of one update of the model $\theta' = \theta - \alpha \nabla_{\theta} \mathcal{L}(f_{\theta}(\tilde{\mathbf{x}}'), \tilde{\mathbf{y}}')$, through which we then backpropagate to update the synthetic labels $\tilde{\mathbf{y}} \leftarrow \tilde{\mathbf{y}} - \beta \nabla_{\tilde{\mathbf{y}}} \mathcal{L}(f_{\theta'}(\mathbf{x}_t'), \mathbf{y}_t')$. We perform a standard update of the model after updating the synthetic labels, which is more of a technical detail about how it is implemented rather than needed in theory as it could be combined with the inner-loop update. The method is otherwise similar to our first-order ridge regression method, which is summarized in Algorithm 1, together with our notation. Note that examples from the target dataset are used when updating the synthetic labels $\tilde{\mathbf{y}}$, but for updating the model θ we only use synthetic labels and the base examples.

After each update of the labels, we normalize them so that they represent a valid probability distribution. This makes them interpretable and has led to improvements compared to unnormalized labels.

Intuition. We analysed how the synthetic labels are meta-learned by the second-order algorithm for a simple one-layer model θ , with a sigmoid output unit and two classes (details are in the supplementary). The meta-gradients are: $\nabla_{\tilde{\mathbf{y}}} \mathcal{L}(f_{\theta'}(\mathbf{x}_t'), \mathbf{y}_t') = \alpha (\sigma(\theta'^T \mathbf{x}_t') - \mathbf{y}_t') \mathbf{x}_t'^T \tilde{\mathbf{x}}'$.

This shows that synthetic labels are updated proportionally to the similarity of the target dataset examples \mathbf{x}_t' and base examples $\tilde{\mathbf{x}}'$ as well as the difference between the predictions and true target set labels. Thus synthetic labels capture the different degrees of similarity between a base example and examples from different classes in the target dataset. For example, in cross-dataset, the KMNIST ‘Ya’  has no corresponding English symbol, but could be learned by partially assigning its label to similar looking English ‘X’’s and ‘R’’s.

First-Order Version with Ridge Regression. To avoid second-order gradients, we propose a first-order version that uses pseudo-gradient generated via a closed form solution to ridge regression. Ridge regression layers have previously been used for few-shot learning (Bertinetto et al. 2019) *within* minibatch. However, we extend it to learn global weights that persist across minibatches. Ridge regression can be defined and solved as:

$$\begin{aligned} W_l &= \arg \min_W \|XW - Y\|^2 + \lambda \|W\|^2 \\ &= (X^T X + \lambda I)^{-1} X^T Y, \end{aligned} \quad (2)$$

where X are the image features, Y are the labels, W are the ridge regression weights and λ is the regularization parameter. Following Bertinetto et al. (2019), we use Woodbury formula (Petersen and Pedersen 2012):

$$W_l = X^T (X X^T + \lambda I)^{-1} Y, \quad (3)$$

which allows us to use matrix $X X^T$ with dimensionality depending on the square of the number of inputs (minibatch size) rather than the square of the input embedding size. The embedding size is typically significantly larger than the size of the minibatch, so it would make matrix inversion costly. While ridge regression (RR) is obviously oriented at regression problems, it has been shown (Bertinetto et al. 2019) to work well for classification when regressing label vectors.

Ridge Regression with Pseudo-Gradients. We use a RR layer as the final output layer of our base network – we decompose the original model θ used for the second-order version into feature extractor θ and RR classifier w . RR solves for the optimal (local) weights w_l that classify the features of the current minibatch examples. We exploit this local minibatch solution by taking a pseudo-gradient step that updates global weights w as $w \leftarrow (1 - \alpha)w + \alpha w_l$, with α being the pseudo-gradient step size. We can understand this as a pseudo-gradient as it corresponds to the step $w \leftarrow w - \alpha(w - w_l)$. We can then update the synthetic labels by back-propagating through local weights w_l . Subsequent feature extractor updates on θ avoid second-order gradients. The full process is summarised in Algorithm 1.

Algorithm 1 Label distillation with ridge regression (RR)

```

1: Input:  $\tilde{\mathbf{x}}$ :  $N$  unlabeled examples from the base dataset;  $(\mathbf{x}_t, \mathbf{y}_t)$ : labeled examples from the target dataset;  $\beta$ : step size;  $\alpha$ : pseudo-gradient step size;  $n_o, n_i$ : outer (resp. inner) loop batch size;  $C$  number of classes in the target dataset
2: Output: distilled labels  $\tilde{\mathbf{y}}$  and a reasonable number of training steps  $T_i$ 
3:  $\tilde{\mathbf{y}} \leftarrow 1/C$  //Uniformly initialize synthetic labels
4:  $\theta \sim p(\theta)$  //Randomly initialize feature extractor parameters
5:  $w \leftarrow 0$  // Initialize global RR classifier weights
6: while  $\tilde{\mathbf{y}}$  not converged do
7:    $(\tilde{\mathbf{x}}', \tilde{\mathbf{y}}') \sim (\tilde{\mathbf{x}}, \tilde{\mathbf{y}})$  //Sample a minibatch of  $n_i$  base examples
8:    $(\mathbf{x}'_t, \mathbf{y}'_t) \sim (\mathbf{x}_t, \mathbf{y}_t)$  //Sample a minibatch of  $n_o$  target examples
9:    $w_l = \arg \min_{w_l} \mathcal{L}(f_{w_l}(f_\theta(\tilde{\mathbf{x}}')), \tilde{\mathbf{y}}')$  // Solve RR problem
10:   $w \leftarrow (1 - \alpha)w + \alpha w_l$  //Update global RR classifier weights
11:   $\tilde{\mathbf{y}} \leftarrow \tilde{\mathbf{y}} - \beta \nabla_{\tilde{\mathbf{y}}} \mathcal{L}(f_w(f_\theta(\mathbf{x}'_t)), \mathbf{y}'_t)$  //Update synthetic labels with target loss
12:   $\theta \leftarrow \theta - \beta \nabla_\theta \mathcal{L}(f_w(f_\theta(\tilde{\mathbf{x}}')), \tilde{\mathbf{y}}')$  //Update feature extractor
13:  if  $\mathcal{L}(f_w(f_\theta(\mathbf{x}_t)), \mathbf{y}_t)$  did not improve then
14:     $\theta \sim p(\theta)$  //Reset feature extractor
15:     $w \leftarrow 0$  // Reset global RR classifier weights
16:     $T_i \leftarrow$  iterations since previous reset //Record time to overfit
17:  end if
18: end while

```

4 Experiments

We perform two main types of experiments: (1) within-dataset distillation, when the base examples come from the target dataset and (2) cross-dataset distillation, when the base examples come from a different but related dataset. The dataset should be related because if there is a large shift in the domain (e.g. from characters to photos), then the feature extractor trained on the base examples would generalize poorly to the target dataset. We use MNIST, CIFAR-10 and CIFAR-100 for the task of within-dataset distillation, while for cross-dataset distillation we use EMNIST (“English letters”), KMNIST, Kuzushiji-49 (both “Japanese letters”), MNIST (digits), CUB (birds) and CIFAR-10 (general objects). Details of these datasets are in the supplementary.

4.1 Experimental Settings

Monitoring Overfitting. We use parameters N_M, N_W to say over how many iterations to calculate the moving average and how many iterations to wait before reset since the best moving average value. We select $N_M = N_W$ and use a value of 50 steps in most cases, while we use 100 for CIFAR-100 and Kuzushiji-49, and 200 for other larger-scale experiments (more than 100 base examples). These parameters do not affect the total number of iterations.

Early Stopping for Learning Synthetic Labels. We update the synthetic labels for a given number of epochs and then select the best labels to use based on the validation performance. For this, we train a new model from scratch using the current distilled labels and the associated base examples and then evaluate the model on the validation part of the target set. We randomly set aside about 10-15% (depending on the dataset) of the training data for validation.

Models. We use LeNet (LeCun et al. 1998) for MNIST and similar experiments, and AlexNet (Krizhevsky,

Sutskever, and Hinton 2012) for CIFAR-10, CIFAR-100 and CUB. Both models are identical to the ones used in (Wang et al. 2018). In a fully supervised setting they achieve about 99% and 80% test accuracy on MNIST and CIFAR-10.

Selection of Base Examples. The base examples are selected randomly, using a shared random seed for consistency across scenarios. Our baseline models use the same random seed as the distillation models, so they share base examples for fair comparison. For within-dataset label distillation, we create a balanced set of base examples, so each class has the same number of base examples. For cross-dataset label distillation, we do not consider the original classes of base examples. The size of the label space and the labels are different in the source and the target problem. Our additional analysis (Tables 6 and 7 in the supplementary) has shown that the specific random set of base examples does not have a significant impact on the success of label distillation.

Further Details. Outer loop minibatch size is $n_o = 1024$ examples, while the inner minibatch size n_i depends on the number of base examples used. When using 100 or more base examples, we select a minibatch of 50 examples, except for CIFAR-100 for which we use 100 examples. For 10, 20 and 50 base examples our minibatch sizes are 10, 10 and 25. We optimize the synthetic labels and the model itself using Adam optimizer with the default parameters ($\beta = 0.001$). Most of our models are trained for 400 epochs, while larger-scale models (more than 100 base examples and CIFAR-100) are trained for 800 epochs. Smaller-scale Kuzushiji-49 experiments are trained for 100 epochs, while larger-scale ones use 200 epochs. Epochs are calculated based on the number of target set examples, rather than base examples. In the second-order version, we perform one inner-loop step update, using a learning rate of $\alpha = 0.01$. We back-propagate through the inner-loop update when updating the synthetic labels (meta-knowledge), but not when

	Base examples	10	20	50	100	200	500
MNIST	LD	60.89 \pm 3.20	74.37 \pm 1.27	82.26 \pm 0.88	87.27 \pm 0.69	91.47 \pm 0.53	93.30 \pm 0.31
	Baseline	48.35 \pm 3.03	62.60 \pm 3.33	75.07 \pm 2.40	82.06 \pm 1.75	85.95 \pm 0.98	92.10 \pm 0.43
	Baseline LS	51.22 \pm 3.18	64.14 \pm 2.57	77.94 \pm 1.26	85.95 \pm 1.09	90.10 \pm 0.60	94.75 \pm 0.29
	LD RR	64.57 \pm 2.67	75.98 \pm 1.00	82.49 \pm 0.93	87.85 \pm 0.43	88.88 \pm 0.28	89.91 \pm 0.33
	Baseline RR	52.53 \pm 2.61	60.44 \pm 1.97	74.85 \pm 2.37	81.40 \pm 2.11	87.03 \pm 0.69	92.10 \pm 0.80
	Baseline RR LS	51.53 \pm 2.42	60.91 \pm 1.78	76.26 \pm 1.80	83.13 \pm 1.41	87.94 \pm 0.67	93.48 \pm 0.61
	DD				79.5 \pm 8.1		
CIFAR-10	SLDD				82.7 \pm 2.8		
	LD	25.69 \pm 0.72	30.00 \pm 0.86	35.36 \pm 0.64	38.33 \pm 0.44	41.05 \pm 0.71	42.45 \pm 0.40
	Baseline	14.29 \pm 1.40	16.80 \pm 0.72	20.75 \pm 1.05	25.76 \pm 1.04	31.53 \pm 1.02	38.33 \pm 0.75
	Baseline LS	13.22 \pm 1.22	18.36 \pm 0.65	22.81 \pm 0.71	27.27 \pm 0.68	33.62 \pm 0.81	39.22 \pm 1.12
	LD RR	25.07 \pm 0.69	29.83 \pm 0.46	35.23 \pm 0.64	37.94 \pm 1.22	41.17 \pm 0.33	43.16 \pm 0.47
	Baseline RR	13.37 \pm 0.79	17.08 \pm 0.31	19.85 \pm 0.51	24.65 \pm 0.47	28.97 \pm 0.74	36.31 \pm 0.49
	Baseline RR LS	13.82 \pm 0.85	16.95 \pm 0.52	20.00 \pm 0.57	24.84 \pm 0.60	29.28 \pm 0.56	35.73 \pm 1.02
DD					36.8 \pm 1.2		
	SLDD				39.8 \pm 0.8		

Table 1: Within-dataset distillation recognition accuracy (%). Our label distillation (LD) outperforms prior Dataset Distillation (Wang et al. 2018) (DD) and SLDD (Sucholutsky and Schonlau 2019), and scales to synthesizing more examples.

subsequently updating the model θ with Adam optimizer. In the first-order version, we use a pseudo-gradient step size of 0.01 and λ of 1.0. We calibrate the regression weights by scaling them with a value learned during training with the specific set of base examples and distilled labels. Our tables report the mean test accuracy and standard deviation (%) across 20 models trained from scratch using the base examples and synthetic labels.

4.2 Within-Dataset Distillation

We compare our label distillation (LD) to previous dataset distillation (DD) and soft-label dataset distillation (SLDD) on MNIST and CIFAR-10. We also establish new baselines that take true labels from the target dataset and otherwise are trained in the same way as LD models. RR baselines use RR and pseudo-gradient for consistency with LD RR (overall network architecture remains the same as in the second-order approach). In addition, we include baselines that use label smoothing (LS) (Szegedy et al. 2016) with a smoothing parameter of 0.1 as suggested in (Pereyra et al. 2017). The number of training steps for our baselines is optimized using the validation set, by training a model for various numbers of steps between 10 and 1000 and measuring the validation set accuracy (up to 1700 steps are used for cases with more than 100 base examples). The results in Table 1 show that LD significantly outperforms previous work on MNIST. This is in part due to LD enabling the use of more steps (LD estimates $T_i \approx 200 - 300$ steps vs fixed 3 epochs of 10 steps in LD and SLDD). Our improved baselines are also competitive, and outperform the prior baselines in Wang et al. (2018) due to taking more steps. However, since Wang et al. (2018); Sucholutsky and Schonlau (2019) do not scale to more steps, this is a reasonable comparison. The standard uniform label smoothing baseline works well on MNIST for a large number of base examples, where the problem anyway approaches one of conventional supervised learning.

However, this strategy has not shown to be effective enough for CIFAR-10, where synthetic labels are the best. Importantly, in the most intensively distilled regime of 10 examples, LD clearly outperforms all competitors. We provide an analysis of the labels learned by our method in Section 4.5. For CIFAR-10 our results also improve on the original DD result. In this experiment, our second-order algorithm performs similarly to our RR pseudo-gradient strategy.

LD	11.46 \pm 0.39
Baseline	3.51 \pm 0.31
Baseline LS	4.07 \pm 0.23
LD RR	10.80 \pm 2.36
Baseline RR	3.00 \pm 0.39
Baseline RR LS	3.65 \pm 0.28

Table 2: CIFAR-100 within-dataset distillation recognition accuracy (%). One example per class.

We further show in Table 2 that our distillation approach scales to a significantly larger number of classes than 10 by application to the CIFAR-100 benchmark. As before, we establish new baseline results that use the original labels (or their smoother alternatives) of the same images as those used as base examples in distillation. We use the validation set to choose a suitable number of steps for training a baseline, allowing up to 1000 steps, which is significantly more than what is typically used by LD. The results show our distillation method leads to clear improvements over the baseline.

4.3 Cross-Dataset Task

For cross-dataset distillation, we considered four scenarios: from EMNIST letters to MNIST digits, from EMNIST letters (“English”) to Kuzushiji-MNIST or Kuzushiji-49 characters (“Japanese”) and from CUB bird species to CIFAR-10

Base examples	10	20	50	100	200	500
E → M (LD)	36.13 ± 5.51	57.82 ± 1.91	69.21 ± 1.82	77.09 ± 1.66	83.67 ± 1.43	86.02 ± 1.00
E → M (LD RR)	56.08 ± 2.88	67.62 ± 3.03	80.80 ± 1.44	82.70 ± 1.33	84.44 ± 1.18	86.79 ± 0.76
E → K (LD)	31.90 ± 2.82	39.88 ± 1.98	47.93 ± 1.38	51.91 ± 0.85	57.46 ± 1.37	59.84 ± 0.80
E → K (LD RR)	34.35 ± 3.37	46.67 ± 1.66	53.13 ± 1.88	57.02 ± 1.24	58.01 ± 1.28	63.77 ± 0.71
B → C (LD)	26.86 ± 0.97	28.63 ± 0.86	31.21 ± 0.74	34.02 ± 0.66	38.39 ± 0.56	38.12 ± 0.41
B → C (LD RR)	26.50 ± 0.54	28.95 ± 0.47	32.23 ± 3.59	32.19 ± 7.89	36.55 ± 6.32	38.46 ± 6.97
E → K-49 (LD)	7.37 ± 1.01	9.79 ± 1.23	17.80 ± 0.78	19.17 ± 1.27	22.78 ± 0.98	23.99 ± 0.81
E → K-49 (LD RR)	10.48 ± 1.26	14.84 ± 1.83	21.59 ± 1.87	20.86 ± 1.81	24.59 ± 2.26	24.72 ± 1.78

Table 3: Cross-dataset distillation recognition accuracy (%). Datasets: E = EMNIST, M = MNIST, K = KMNIST, B = CUB, C = CIFAR-10, K-49 = Kuzushiji-49.

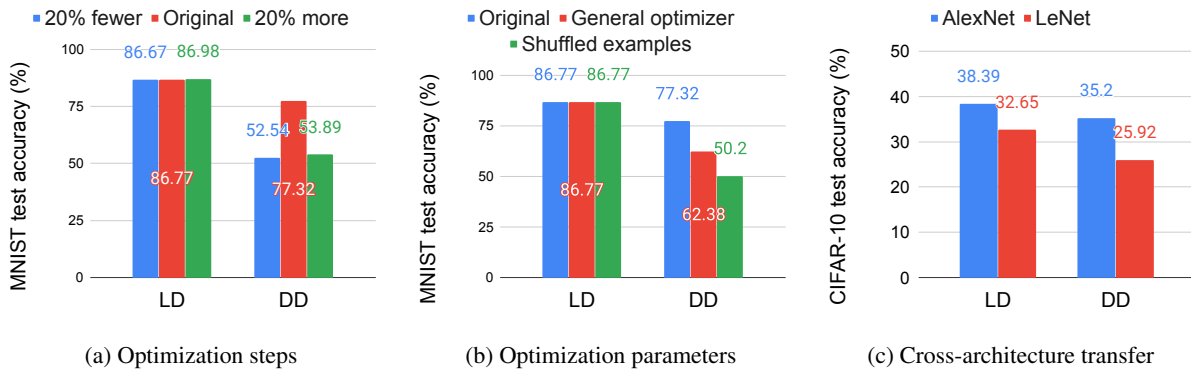


Figure 2: LD distilled datasets are more agnostic to optimization steps, hyperparameters, and network architecture than DD.

general categories. The results in Table 3 show we are able to distill labels on examples of a different source dataset and achieve surprisingly good performance on the target problem, given that no target data is used when training these models. In contrast, directly applying a trained source-task model to the target without distillation unsurprisingly leads to chance performance (about 2% test accuracy for Kuzushiji-49 and 10% for all other cases). These results show we can indeed distill the knowledge of one dataset into base examples from a different but related dataset through crafting synthetic labels. Furthermore, our RR approach surpasses the second-order method in most cases, confirming its value. When using 10 and 20 base examples for Kuzushiji-49, the number of training examples is smaller than the number of classes (49), providing a novel example of *less-than-one-shot learning* where there are fewer examples than classes (Sucholutsky and Schonlau 2020).

4.4 Flexibility of Distilled Datasets

We conduct experiments to verify the flexibility and general applicability of our label-distilled dataset compared to image-distilled alternative by Wang et al. (2018). Namely, we looked at (1) How the number of steps used during meta-testing affects the performance of learning with the distilled data, and in particular sensitivity to deviation from the number of steps used during meta-training of DD and LD. (2) Sensitivity of the models to changes in optimization param-

eters between meta-training + meta-testing. (3) How well the distilled datasets transfer to neural architectures different to those used for training. We used the DD implementation of Wang et al. (2018) for fair evaluation. Figure 2 summarizes the key points, and detailed tables are in the supplementary.

Sensitivity to the Number of Meta-Testing Steps (Figure 2a). A key feature of our method is that it is relatively insensitive to the number of steps used to train a model on the distilled data. Our results from Table 9 show that even if we do 50 steps less or 100 steps more than the number estimated during training (≈ 300), the testing performance does not change significantly. This is in contrast with previous DD and SLDD methods that must be trained for a specific number of steps with optimized learning rates, making them rather inflexible. If the number of steps changes even by as little as 20%, they incur a significant cost in accuracy. Table 10 provides a further analysis of sensitivity of DD.

Sensitivity to Optimization Parameters (Figure 2b). DD uses step-wise meta-optimized learning rates to maximize accuracy. Our analysis in Table 11 shows that if we use an average of the optimized learning rate rather than the specific value in each step (more general optimizer), the performance decreases significantly. Further, original DD relies on training the distilled data in a fixed sequence, and our analysis in Table 12 shows changing the order of examples leads to a large decrease in accuracy. Our LD method by design

does not depend on the specific order of examples, and it can be used with off-the-shelf learning optimizers such as Adam to train the model, rather than with optimizers with learning rates specific to the example and step.

Transferability of Labels Across Architectures (Figure 2c). We study the impact of distilling the labels using AlexNet and then training AlexNet, LeNet and ResNet-18 using the distilled labels. We establish new baselines for the additional architectures, using a number of steps chosen based on the validation set. Results in Tables 13 and 14 suggest our labels are helpful in both within and across dataset distillation scenarios. This suggests that even if we relabel a dataset with one label space to solve a different problem, the labels generalize to a new architecture and lead to improvements over the baselines. We have done experiments with original DD to find how robust it is to the change of architecture (Table 15). As expected, there is a large decrease in accuracy, but the results are better than the baselines they report (Wang et al. 2018), so their synthetic images are somewhat transferable when we train the model with the specific order of examples and optimized learning rates. However, our LD method incurs a smaller decrease in accuracy, suggesting better transferability across architectures.

4.5 Further Analysis

Training Time. In Table 4 we compare training times of our framework and the original DD (using the same settings and hardware). Besides evaluating LD, we also use our meta-learning algorithm to implement an image-distillation strategy for direct comparison with the original DD. The results show our online approach significantly accelerates training. Our DD is comparable to LD, and both are faster than original DD. However, we focus on LD because our version of DD was relatively unstable and led to worse performance than LD, perhaps because learning synthetic images is more complex than synthetic labels. This shows we need both the labels and our re-initializing strategy.

	MNIST	CIFAR-10
DD	116	205
LD	61	86
LD (RR)	65	98
Our DD	67	96
Our DD (RR)	72	90

Table 4: Comparison of training times of DD (Wang et al. 2018) and our LD (minutes).

Analysis of Synthetic Labels. We have analysed to what extent the synthetic labels learn the true label and how this differs between our second-order and RR methods (Figures 8 and 9 in the supplementary). The results for a MNIST experiment with 100 base examples show the second-order method recovers the true value to about 84% on average, so it could be viewed as non-uniform label smoothing with meta-learned weights on labels specific to the examples. For the same scenario, RR recovers the true value to about 63%

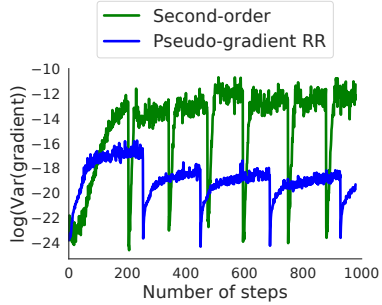


Figure 3: RR-based LD reduces synthetic label meta-gradient variance $\text{Var}[\nabla_{\tilde{y}} \mathcal{L}]$.

on average, suggesting RR leads to more complex labels that may better capture the different amounts of similarity of base examples to examples from different classes in the target dataset. This is also supported by visually similar digits such as 4 and 9 receiving more weight compared to other combinations. For CIFAR-10, the labels are significantly more complex, indicating non-trivial information is embedded into the synthetic labels. For cross-dataset LD (EMNIST base examples with KMNIST and MNIST target respectively), Figure 10 suggests LD can be understood as learning labels such that the base examples’ label-weighted combination resembles the images from the target class. Examples of synthetic labels for both within and cross-dataset LD are also included in the supplementary.

Pseudo-Gradient Analysis. To understand the superior performance of our RR method, we analysed the variances of meta-gradients obtained by our second-order and pseudo-gradient methods. Results in Figure 3 show our pseudo-gradient RR method obtains a significantly lower variance of meta-knowledge gradients, leading to more stable and effective training.

Discussion. LD provides a more effective and more flexible distillation approach than prior work. This brings us one step closer to the vision of leveraging distilled data to accelerate model training, or design – such as architecture search (Elsken, Metzen, and Hutter 2019). Currently we only explicitly randomize over network initializations during training. In future work we believe our strategy of multi-step training and reset at convergence could be used with other factors, such as randomly selected network architectures to further improve cross-network generalisation performance.

5 Conclusion

We have introduced a new label distillation algorithm for distilling the knowledge of a large dataset into synthetic labels of a few base examples from the same or a different dataset. Our method improves on prior dataset distillation results, scales better to larger problems, and enables novel settings such as cross-dataset distillation. Most importantly, it is significantly more flexible in terms of distilling general purpose datasets that can be used downstream with off-the-shelf optimizers.

Ethics Statement

We propose a flexible and efficient distillation scheme that gets us closer to the goal of practically useful dataset distillation. Dataset distillation could ultimately lead to a beneficial impact in terms of researcher’s time efficiency by enabling faster experimentation when training on small distilled datasets. Perhaps more importantly, it could reduce the environmental impact of AI research and development by reduction of energy costs (Schwartz et al. 2019). However, our results are still not strong enough yet. For this goal to be realised better distillation methods leading to more accurate downstream models need to be developed.

In the future, label distillation could speculatively provide a useful tool for privacy preserving learning (Al-Rubaie and Chang 2019), for example in situations where organizations want to learn from user’s data. A company could provide a small set of public (source) data to a user, who performs cross-dataset distillation using their private (target) data to train a model. The user would then return the distilled labels on the public data, which would allow the company to recreate the user’s model. In this way the knowledge from the user’s training could be obtained by the company in the form of distilled labels – without directly sending any private data, or trained model that could be a vector for memorization attacks (Carlini et al. 2019).

On the negative side, detecting and understanding the impact of bias in datasets is an important yet already very challenging issue for machine learning. The impact of dataset distillation on any underlying biases in the data is completely unclear. If people were to train models on distilled datasets in the future, it would be important to understand the impact of distillation on data biases.

Source Code

We provide a PyTorch implementation of our approach at <https://github.com/ondrejbohdal/label-distillation>.

Acknowledgments

This work was supported in part by the EPSRC Centre for Doctoral Training in Data Science, funded by the UK Engineering and Physical Sciences Research Council (grant EP/L016427/1) and the University of Edinburgh.

References

Al-Rubaie, M.; and Chang, J. M. 2019. Privacy-preserving machine learning: threats and solutions. *IEEE Security and Privacy* 17(2): 49–58.

Angelova, A.; Abu-Mostafa, Y.; and Perona, P. 2005. Pruning training sets for learning of object categories. In *CVPR*.

Balaji, Y.; Sankaranarayanan, S.; and Chellappa, R. 2018. MetaReg: towards domain generalization using meta-regularization. In *NeurIPS*.

Bertinetto, L.; Henriques, J.; Torr, P. H. S.; and Vedaldi, A. 2019. Meta-learning with differentiable closed-form solvers. In *ICLR*.

Carlini, N.; Liu, C.; Erlingsson, U.; Kos, J.; and Song, D. 2019. The secret sharer: evaluating and testing unintended memorization in neural networks. In *USENIX Security Symposium*.

Clanuwat, T.; Kitamoto, A.; Lamb, A.; Yamamoto, K.; and Ha, D. 2018. Deep learning for classical Japanese literature. In *NeurIPS Workshop on Machine Learning for Creativity and Design*.

Cohen, G.; Afshar, S.; Tapson, J.; and van Schaik, A. 2017. EMNIST: an extension of MNIST to handwritten letters. In *arXiv*.

Elsken, T.; Metzen, J. H.; and Hutter, F. 2019. Neural architecture search: a survey. *Journal of Machine Learning Research* 20: 1–21.

Farquhar, G.; Whiteson, S.; and Foerster, J. 2019. Loaded DiCE: Trading off Bias and Variance in Any-Order Score Function Estimators for Reinforcement Learning. In *NeurIPS*.

Felzenszwalb, P. F.; Girshick, R. B.; McAllester, D.; and Ramanan, D. 2010. Object detection with discriminatively trained part-based models. *IEEE Transactions on Pattern Analysis and Machine Intelligence* 32(9): 1627–1645.

Finn, C.; Abbeel, P.; and Levine, S. 2017. Model-agnostic meta-learning for fast adaptation of deep networks. In *ICML*.

Hinton, G.; Vinyals, O.; and Dean, J. 2014. Distilling the knowledge in a neural network. In *NIPS*.

Hospedales, T.; Antoniou, A.; Micaelli, P.; and Storkey, A. 2020. Meta-learning in neural networks: a survey. In *arXiv*.

Krizhevsky, A. 2009. Learning multiple layers of features from tiny images. Technical report.

Krizhevsky, A.; Sutskever, I.; and Hinton, G. E. 2012. ImageNet classification with deep convolutional neural networks. In *NIPS*.

LeCun, Y.; Bottou, L.; Bengio, Y.; and Haffner, P. 1998. Gradient-based learning applied to document recognition. *Proceedings of the IEEE* 86(11): 2278–2324.

Lee, K.; Maji, S.; Ravichandran, A.; and Soatto, S. 2019. Meta-learning with differentiable convex optimization. In *CVPR*.

Li, Y.; Yang, Y.; Zhou, W.; and Hospedales, T. M. 2019. Feature-critic networks for heterogeneous domain generalization. In *ICML*.

Liu, H.; Socher, R.; and Xiong, C. 2019. Taming MAML: Efficient Unbiased Meta-Reinforcement Learning. In *ICML*.

Lorraine, J.; Vicol, P.; and Duvenaud, D. 2020. Optimizing Millions of Hyperparameters by Implicit Differentiation. In *AISTATS*.

Luketina, J.; Berglund, M.; Klaus Greff, A.; and Raiko, T. 2016. Scalable Gradient-Based Tuning of Continuous Regularization Hyperparameters. In *ICML*.

Maclaurin, D.; Duvenaud, D.; and Adams, R. P. 2015. Gradient-based Hyperparameter Optimization through Reversible Learning. In *ICML*.

Micaelli, P.; and Storkey, A. 2019. Zero-shot knowledge transfer via adversarial belief matching. In *NeurIPS*.

Nichol, A.; Achiam, J.; and Schulman, J. 2018. On first-order meta-learning algorithms. In *arXiv*.

Olvera-López, J. A.; Carrasco-Ochoa, J. A.; Martínez-Trinidad, J. F.; and Kittler, J. 2010. A review of instance selection methods. *Artificial Intelligence Review* 34(2): 133–143.

Pereyra, G.; Tucker, G.; Chorowski, J.; Kaiser, L.; and Hinton, G. 2017. Regularizing neural networks by penalizing confident output distributions. In *arXiv*.

Petersen, K. B.; and Pedersen, M. S. 2012. The matrix cookbook. Technical report.

Schwartz, R.; Dodge, J.; Smith, N. A.; and Etzioni, O. 2019. Green AI. In *arXiv*.

Sener, O.; and Savarese, S. 2018. Active learning for convolutional neural networks: A core-set approach. In *ICLR*.

Shleifer, S.; and Prokop, E. 2019. Proxy Datasets for Training Convolutional Neural Networks. In *arXiv*.

Sucholutsky, I.; and Schonlau, M. 2019. Soft-label dataset distillation and text dataset distillation. In *arXiv*.

Sucholutsky, I.; and Schonlau, M. 2020. 'Less Than One'-Shot Learning: Learning N Classes From $M < N$ Samples. In *arXiv*.

Szegedy, C.; Vanhoucke, V.; Ioffe, S.; and Shlens, J. 2016. Rethinking the Inception architecture for computer vision. In *CVPR*.

Tsang, I. W.; Kwok, J. T.; and Cheung, P.-M. 2005. Core vector machines: fast SVM training on very large data sets. *Journal of Machine Learning Research* 6: 363–392.

Wah, C.; Branson, S.; Welinder, P.; Perona, P.; and Belongie, S. 2011. The Caltech-UCSD Birds-200-2011 dataset. Technical report.

Wang, T.; Zhu, J.-Y.; Torralba, A.; and Efros, A. A. 2018. Dataset distillation. In *arXiv*.

A Datasets

We use MNIST (LeCun et al. 1998), EMNIST (Cohen et al. 2017), KMNIST and Kuzushiji-49 (Clanuwat et al. 2018), CIFAR-10 and CIFAR-100 (Krizhevsky 2009), and CUB (Wah et al. 2011) datasets. Example images are shown in Figure 4. MNIST includes images of 70000 handwritten digits that belong into 10 classes. EMNIST dataset includes various characters, but we choose EMNIST letters split that includes only letters. Lowercase and uppercase letters are combined together into 26 balanced classes (145600 examples in total). KMNIST (Kuzushiji-MNIST) is a dataset that includes images of 10 classes of cursive Japanese (*Kuzushiji*) characters and is of the same size as MNIST. Kuzushiji-49 is a larger version of KMNIST with 270912 examples and 49 classes. CIFAR-10 includes 60000 colour images of various general objects, for example airplanes, frogs or ships. As the name indicates, there are 10 classes. CIFAR-100 is like CIFAR-100, but has 100 classes with 600 images for each of them. Every class belongs to one of 20 superclasses which represent more general concepts. CUB includes colour images of 200 bird species. The number of images is relatively small, only 11788. All datasets except Kuzushiji-49 are balanced or almost balanced.

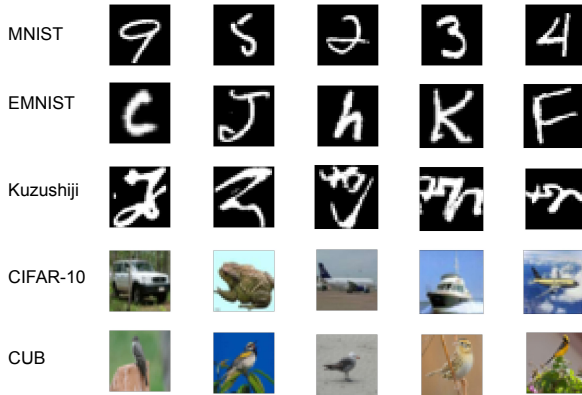


Figure 4: Example images from the different datasets that we use.

B Analysis of Simple One-Layer Case

In this section we analyse how synthetic labels are meta-learned in the case of a simple one-layer model with sigmoid output layer σ , second-order approach and binary classification problem. We will consider one example at a time for simplicity. The model has weights θ and gives prediction $\hat{y} = \sigma(\theta^T \mathbf{x})$ for input image \mathbf{x} with true label y . We use binary cross-entropy loss: $\mathcal{L}(\hat{y}, y) = y \log \hat{y} + (1 - y) \log(1 - \hat{y})$.

As part of the algorithm, we first update the base model, using the current base example and synthetic label:

$$\theta' = \theta - \alpha \nabla_{\theta} \mathcal{L}(\sigma(\theta^T \tilde{\mathbf{x}}), \tilde{y}),$$

after which we update the synthetic label:

$$\tilde{y} \leftarrow \tilde{y} - \beta \nabla_{\tilde{y}} \mathcal{L}(\sigma(\theta'^T \mathbf{x}_t), y_t).$$

Notation: $\tilde{\mathbf{x}}$ is the base example, \tilde{y} is the synthetic label, α is the inner-loop learning rate, β is the outer-loop learning rate, \mathbf{x}_t is the target set example, y_t is the label of the target set example and θ describes the model weights.

Our goal is to intuitively interpret the update of the synthetic label, which uses the gradient $\nabla_{\tilde{y}} \mathcal{L}(\sigma(\theta'^T \mathbf{x}_t), y_t)$.

We will repeatedly use the chain rule and the fact that

$$\frac{\partial \sigma(x)}{\partial x} = \sigma(x)(1 - \sigma(x)).$$

Moreover, we will use the following result (for binary cross-entropy loss \mathcal{L} introduced earlier):

$$\begin{aligned} \frac{\partial \mathcal{L}(\sigma(\theta^T \mathbf{x}), y)}{\partial \theta} &= \frac{\partial \mathcal{L}(\sigma(\theta^T \mathbf{x}), y)}{\partial \sigma(\theta^T \mathbf{x})} \frac{\partial \sigma(\theta^T \mathbf{x})}{\partial \theta} \\ &= (y - \sigma(\theta^T \mathbf{x})) \mathbf{x} \end{aligned}$$

Now we derive an intuitive formula for the gradient used for updating the synthetic label:

$$\begin{aligned} \frac{\partial \mathcal{L}(\sigma(\theta'^T \mathbf{x}_t), y_t)}{\partial \tilde{y}} &= \frac{\partial \mathcal{L}(\hat{y}_t, y_t)}{\partial \tilde{y}} \\ &= \left(\frac{\partial \mathcal{L}(\hat{y}_t, y_t)}{\partial \hat{y}_t} \frac{\partial \hat{y}_t}{\partial \theta'} \right)^T \frac{\partial \theta'}{\partial \tilde{y}} \\ &= \left(\frac{\partial \mathcal{L}(\hat{y}_t, y_t)}{\partial \hat{y}_t} \frac{\partial \hat{y}_t}{\partial \theta'} \right)^T \frac{\partial (\theta - \alpha \nabla_{\theta} \mathcal{L}(\sigma(\theta^T \tilde{\mathbf{x}}), \tilde{y}))}{\partial \tilde{y}} \\ &= \left(\frac{\partial \mathcal{L}(\hat{y}_t, y_t)}{\partial \hat{y}_t} \frac{\partial \hat{y}_t}{\partial \theta'} \right)^T \frac{\partial (\theta - \alpha (\tilde{y} - \sigma(\theta^T \tilde{\mathbf{x}})) \tilde{\mathbf{x}})}{\partial \tilde{y}} \\ &= \left(\frac{\partial \mathcal{L}(\hat{y}_t, y_t)}{\partial \hat{y}_t} \frac{\partial \hat{y}_t}{\partial \theta'} \right)^T (-\alpha \tilde{\mathbf{x}}) \\ &= ((y_t - \hat{y}_t) \mathbf{x}_t)^T (-\alpha \tilde{\mathbf{x}}) \\ &= \alpha (\sigma(\theta'^T \mathbf{x}_t) - y_t) \mathbf{x}_t^T \tilde{\mathbf{x}} \end{aligned}$$

The next step is to interpret the update rule. The update is proportional to the difference between the prediction on the target set and the true label ($\sigma(\theta'^T \mathbf{x}_t) - y_t$) as well as to the similarity between the target set example and the base example ($\mathbf{x}_t^T \tilde{\mathbf{x}}$). This suggests the synthetic labels are updated so that they capture the different amount of similarity of a base example to examples from different classes in the target dataset. A similar analysis can also be done for our RR method – in such case the result would be similar and would include a further proportionality constant dependent on the base examples (not affecting the intuitive interpretation).

C Additional Experimental Details

Normalization. We normalize greyscale images using the standardly used normalization for MNIST (mean of 0.1307 and standard deviation of 0.3081). All our greyscale images are of size 28×28 . Colour images are normalized using CIFAR-10 normalization (means of about 0.4914, 0.4822, 0.4465, and standard deviations of about 0.247, 0.243, 0.261 across channels). All colour images are reshaped to be of size 32×32 .

Computational Resources. Each experiment was done on a single GPU, in almost all cases NVIDIA 2080 Ti. Shorter (400 epochs) experiments took about 1 or 2 hours to run, while longer (800 epochs) experiments took between 2 and 4 hours.

In addition, Figure 5 illustrates the difference between a standard model used for second-order label distillation and a model that uses global ridge regression classifier weights (used for first-order RR label distillation). The two models are almost identical – only the final linear layer is different.

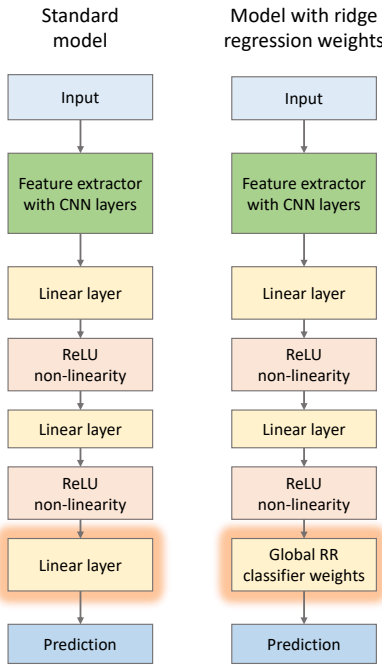


Figure 5: Comparison of a standard model used for second-order label distillation and a model that uses global ridge regression classifier weights (used for first-order RR label distillation).

D Additional Experiments

Stability and Dependence on Choice of Base Examples. To evaluate the consistency of our results, we repeat the entire pipeline and report the results in Table 5. In the previous experiments, we used one randomly chosen but fixed set of base examples per source task. We investigate the impact of base example choice by drawing further random base example sets. The results in Table 6 suggest that the impact of base example choice is slightly larger than that of the variability due to the distillation process, but still small overall. Note that the \pm standard deviations in all cases quantify the impact of retraining from different random initializations at meta-test, given a fixed base set and completed distillation. It is likely that if the base examples were not selected randomly, the impact of using specific base examples would be

larger. In fact, future work could investigate how to choose base examples so that learning synthetic labels for them improves the result further. We have tried the following strategy, but the label distillation results remained similar to the previous results (the new results are in Table 7):

- Try 50 randomly selected sets of examples, train a model with each three times (for robustness) and measure the validation accuracy.
- The validation accuracy is measured for various numbers of steps, in most cases we evaluate every 50 steps up to 1000 steps (with some additional small number of steps at the beginning). If there are more than 100 base examples, we allow up to 1700 steps.
- Select the set with the largest mean validation accuracy at any point of training (across the three runs).
- This strategy maximizes the performance of the baselines, but could potentially also help the label distillation since these examples could be generally better for training.

Dependence on Target Dataset Size. Our experiments use a relatively large target dataset (about 50000 examples) for meta-learning. We study the impact of reducing the amount of target data for distillation in Table 8. Using 5000 or more examples (about 10% of the original size) is enough to achieve comparable performance.

Transferability of RR Synthetic Labels to Standard Model Training. When using RR, we train a validation and test model with RR and global classifier weights obtained using pseudo-gradient. In this experiment we study what happens if we create synthetic labels with RR, but do validation and testing with standard models trained from scratch without RR. For a fair comparison, we use the same synthetic labels for training a new RR model and a new standard model. Validation for early stopping is done with a standardly trained model. The results in Table 16 suggest RR labels are largely transferable (even in cross-dataset scenarios), but there is some decrease in performance. Consequently, it is better to learn the synthetic labels using second-order approach if we want to train a standard model without RR during testing (comparing with the results in Table 1, 2 and 3).

Intuition on Cross-Dataset Distillation. To illustrate the mechanism behind cross-dataset distillation, we use the distilled labels to linearly combine base EMNIST example images weighted by their learned synthetic labels in order to estimate a prototypical KMNIST/MNIST target class example as implied by learned LD labels. Although the actual mechanism is more complex than this due to the non-linearity of the neural network, we can qualitatively see individual KMNIST/MNIST target classes are approximately encoded by their linear EMNIST LD prototypes as shown in Figure 10.

E Results of Analysis

Our tables report the mean test accuracy and standard deviation (%) across 20 models trained from scratch using the base examples and synthetic labels. When analysing original DD, 200 randomly initialized models are used.

	Trial 1	Trial 2	Trial 3
MNIST (LD)	87.27 ± 0.69	87.49 ± 0.44	86.77 ± 0.77
MNIST (LD RR)	87.85 ± 0.43	88.31 ± 0.44	88.07 ± 0.46
E \rightarrow M (LD)	77.09 ± 1.66	76.81 ± 1.47	77.10 ± 1.74
E \rightarrow M (LD RR)	82.70 ± 1.33	83.06 ± 1.43	81.46 ± 1.70

Table 5: Repeatability. Label distillation is quite repeatable. Performance change from repeating the whole distillation learning and subsequent re-training is small. We used 100 base examples for these experiments. Datasets: E = EMNIST, M = MNIST.

	Set 1	Set 2	Set 3	Set 4	Set 5
MNIST (LD)	84.91 ± 0.92	87.38 ± 0.81	87.49 ± 0.44	87.12 ± 0.47	85.16 ± 0.48
MNIST (LD RR)	87.82 ± 0.60	88.78 ± 0.57	88.31 ± 0.44	88.40 ± 0.46	87.77 ± 0.60
E \rightarrow M (LD)	79.34 ± 1.36	74.55 ± 1.00	76.81 ± 1.47	78.59 ± 1.05	78.55 ± 1.32
E \rightarrow M (LD RR)	81.67 ± 1.39	83.30 ± 1.38	83.06 ± 1.43	82.62 ± 1.70	83.43 ± 0.98

Table 6: Base example sensitivity. Label distillation has some sensitivity to the specific set of base examples (chosen by a specific random seed), but the sensitivity is relatively low. We used 100 base examples for these experiments. It is likely that label distillation would be more sensitive for a smaller number of base examples.

	Base examples	10	20	50	100	200	500
MNIST	LD	66.96 ± 2.01	74.37 ± 1.65	83.17 ± 1.28	86.66 ± 0.44	90.75 ± 0.49	93.22 ± 0.41
	Baseline	56.60 ± 3.10	64.77 ± 1.90	77.33 ± 2.51	84.86 ± 1.16	88.33 ± 1.04	92.87 ± 0.67
	Baseline LS	60.44 ± 2.05	66.41 ± 2.14	80.54 ± 1.94	86.98 ± 0.99	91.12 ± 0.79	95.56 ± 0.18
	LD RR	71.34 ± 2.19	73.34 ± 1.18	84.66 ± 0.89	88.30 ± 0.46	88.91 ± 0.36	89.73 ± 0.39
	Baseline RR	59.20 ± 2.18	65.22 ± 2.29	77.34 ± 1.68	84.70 ± 0.81	87.87 ± 0.68	92.39 ± 0.53
	Baseline RR LS	60.63 ± 1.64	65.61 ± 1.08	77.39 ± 1.67	85.63 ± 0.95	88.89 ± 0.88	94.33 ± 0.44
	DD				79.5 ± 8.1		
	SLDD				82.7 ± 2.8		
CIFAR-10	LD	26.65 ± 0.94	29.07 ± 0.62	35.03 ± 0.48	38.17 ± 0.36	42.12 ± 0.56	41.90 ± 0.28
	Baseline	17.57 ± 1.63	21.66 ± 0.91	23.59 ± 0.80	27.79 ± 1.01	33.49 ± 0.77	40.44 ± 1.33
	Baseline LS	18.57 ± 0.68	22.91 ± 0.70	24.57 ± 0.83	29.27 ± 0.85	34.83 ± 0.75	40.15 ± 0.66
	LD RR	25.08 ± 0.39	28.17 ± 0.34	34.43 ± 0.38	37.59 ± 1.68	42.48 ± 0.25	44.81 ± 0.26
	Baseline RR	18.42 ± 0.59	21.00 ± 0.73	22.45 ± 0.49	24.46 ± 1.67	30.96 ± 0.49	39.17 ± 0.47
	Baseline RR LS	18.22 ± 0.67	22.31 ± 1.01	22.27 ± 0.75	24.84 ± 2.89	30.74 ± 0.80	38.86 ± 0.88
	DD				36.8 ± 1.2		
	SLDD				39.8 ± 0.8		

Table 7: Optimized base examples: within-dataset distillation recognition accuracy (%). Our label distillation (LD) outperforms prior Dataset Distillation (Wang et al. 2018) (DD) and SLDD (Sucholutsky and Schonlau 2019), and scales to synthesizing more examples. The LD results remained similar to the original results even with optimized base examples.

Target examples	100	500	1000	5000	10000	20000	All
E \rightarrow M (LD)	50.70 ± 2.33	61.92 ± 3.62	57.39 ± 4.58	75.44 ± 1.60	76.79 ± 1.12	77.27 ± 1.25	77.09 ± 1.66
E \rightarrow M (LD RR)	60.67 ± 3.17	72.09 ± 2.40	65.71 ± 3.77	76.83 ± 2.33	80.66 ± 1.97	82.44 ± 1.64	82.70 ± 1.33

Table 8: Dependence on target set size. Around 5000 examples ($\approx 10\%$ of all data) is sufficient. Similarly as before, we used 100 base examples. Using all examples means using 50000 examples.

Steps deviation	- 50	- 20	- 10	+ 0	+ 10	+ 20	+ 50	+ 100
MNIST (LD)	86.67 \pm 0.51	86.91 \pm 0.49	86.88 \pm 0.50	86.77 \pm 0.77	86.54 \pm 0.68	87.05 \pm 0.67	86.98 \pm 0.70	86.59 \pm 0.63
MNIST (LD RR)	88.21 \pm 0.50	88.03 \pm 0.51	88.32 \pm 0.50	88.07 \pm 0.46	88.10 \pm 0.38	87.95 \pm 0.45	87.98 \pm 0.45	87.74 \pm 0.62
E \rightarrow M (LD)	77.28 \pm 1.01	76.88 \pm 1.97	77.26 \pm 1.92	77.10 \pm 1.74	76.40 \pm 2.37	76.76 \pm 2.18	77.80 \pm 1.49	77.81 \pm 1.23
E \rightarrow M (LD RR)	81.84 \pm 1.75	81.64 \pm 1.76	81.45 \pm 2.01	81.46 \pm 1.70	81.55 \pm 1.80	80.96 \pm 1.74	81.34 \pm 1.64	80.73 \pm 2.45

Table 9: Sensitivity to number of training steps at meta-testing. We re-train the model with different numbers of steps than estimated during meta-training. The results show our method is relatively insensitive to the number of steps. The default number of steps T_i (+ 0 column) was estimated as 278 for MNIST (LD), 217 for MNIST (LD RR), 364 steps for E \rightarrow M (LD) and 311 steps for E \rightarrow M (LD RR). Scenario with 100 base examples is reported.

Steps	10	15	20	25	30	35
MNIST	35.65 \pm 11.19	43.25 \pm 11.47	54.85 \pm 12.28	52.54 \pm 11.40	77.32 \pm 5.08	53.89 \pm 10.51
CIFAR-10	21.14 \pm 4.08	22.50 \pm 4.24	27.08 \pm 3.22	28.54 \pm 2.41	35.20 \pm 1.09	28.80 \pm 3.33

Table 10: Sensitivity of original DD to number of steps. DD is very sensitive to using the specific number of steps. We take the first N steps, keep their original learning rates, and assign learning rates of 0 to the remaining steps. When we do 5 more steps than the original (30), we perform the final 5 steps with an average learning rate.

	Learning rate	Optimized	Average of optimized
MNIST	77.32 \pm 5.08	62.38 \pm 13.11	
CIFAR-10	35.20 \pm 1.09	30.59 \pm 3.95	

Table 11: Sensitivity of original DD to learning rates. DD is sensitive to using the specific learning rates.

Order	Original	Shuffled within epoch	Shuffled across epochs
MNIST	77.32 \pm 5.08	50.20 \pm 12.83	62.67 \pm 10.82
CIFAR-10	35.20 \pm 1.09	24.65 \pm 2.16	22.59 \pm 3.23

Table 12: Sensitivity of original DD to order of examples. DD is sensitive to using the specific order of training examples.

Base examples	10	20	50	100	200	500
CIFAR-10 LD						
AlexNet	26.09 \pm 0.58	30.41 \pm 0.81	35.21 \pm 0.50	38.39 \pm 0.62	40.98 \pm 0.50	42.78 \pm 0.29
LeNet	19.33 \pm 2.50	24.17 \pm 1.42	28.14 \pm 1.37	32.65 \pm 1.22	36.60 \pm 1.46	39.67 \pm 0.85
ResNet-18	17.97 \pm 1.23	24.64 \pm 0.92	27.36 \pm 1.07	31.01 \pm 0.84	35.33 \pm 0.97	39.32 \pm 0.61
CIFAR-10 baseline						
AlexNet	14.35 \pm 1.39	16.72 \pm 0.76	21.08 \pm 0.93	25.39 \pm 0.86	31.39 \pm 1.12	37.17 \pm 1.58
LeNet	13.20 \pm 1.86	15.31 \pm 1.09	18.15 \pm 0.82	21.63 \pm 1.45	25.87 \pm 1.26	32.99 \pm 0.86
ResNet-18	13.80 \pm 1.19	18.29 \pm 1.43	20.56 \pm 0.75	23.44 \pm 1.04	28.98 \pm 1.05	33.16 \pm 1.12
CUB to CIFAR-10 LD						
AlexNet	25.95 \pm 0.90	27.73 \pm 1.09	31.00 \pm 0.78	34.99 \pm 0.69	37.83 \pm 0.65	39.44 \pm 0.53
LeNet	20.18 \pm 1.56	23.15 \pm 1.72	26.16 \pm 1.55	28.73 \pm 1.44	30.71 \pm 1.80	35.41 \pm 0.88
ResNet-18	17.12 \pm 1.32	17.80 \pm 1.26	21.22 \pm 1.04	23.38 \pm 0.95	23.39 \pm 0.90	26.71 \pm 0.89

Table 13: Transferability of distilled labels across different architectures (second-order method). The upper part of the table shows performance of various test models when trained on distilled labels synthesised with AlexNet only. The middle part shows the baseline performance of training models with different architectures on true labels. The lower part shows that distilled labels work even in cross-dataset scenario (labels trained with AlexNet only). The results clearly suggest the distilled labels generalize across different architectures.

Base examples	10	20	50	100	200	500
CIFAR-10 LD						
AlexNet	26.78 ± 0.84	29.51 ± 0.41	34.71 ± 0.45	38.29 ± 0.92	41.14 ± 0.37	42.71 ± 0.27
LeNet	20.24 ± 2.06	23.58 ± 1.62	28.05 ± 1.66	30.64 ± 1.47	34.52 ± 1.16	38.75 ± 0.96
ResNet-18	16.63 ± 0.88	17.98 ± 1.38	23.03 ± 1.21	26.66 ± 0.73	31.08 ± 0.92	36.37 ± 0.81
CIFAR-10 baseline						
AlexNet	13.37 ± 0.75	17.20 ± 0.50	19.07 ± 0.75	24.72 ± 0.53	29.94 ± 0.65	36.20 ± 0.97
LeNet	12.33 ± 0.88	14.28 ± 0.74	17.31 ± 0.97	20.61 ± 1.13	24.15 ± 0.98	28.92 ± 0.80
ResNet-18	14.04 ± 1.20	16.60 ± 1.25	18.75 ± 1.17	22.61 ± 1.03	28.03 ± 0.72	33.72 ± 1.74
CUB to CIFAR-10 LD						
AlexNet	26.08 ± 1.14	29.37 ± 0.36	31.46 ± 3.94	35.74 ± 0.81	37.26 ± 1.63	40.94 ± 4.61
LeNet	22.69 ± 2.09	24.42 ± 1.53	26.35 ± 1.26	29.84 ± 1.36	31.68 ± 1.09	35.66 ± 1.98
ResNet-18	16.23 ± 1.44	17.44 ± 0.84	20.06 ± 0.74	23.48 ± 1.00	21.31 ± 0.82	29.86 ± 0.93

Table 14: Transferability of distilled labels across different architectures (RR method). The upper part of the table shows performance of various test models when trained on distilled labels synthetised with AlexNet only. The middle part shows the baseline performance of training models with different architectures on true labels. The lower part shows that distilled labels work even in cross-dataset scenario (labels trained with AlexNet only). The results clearly suggest the distilled labels generalize across different architectures. Note that lower RR results for ResNet-18 may be caused by significantly lower dimensionality of the RR layer (64 features + 1 for bias), while AlexNet and LeNet have 192 features + 1 for bias in the RR layer.

	AlexNet	LeNet
CIFAR-10	35.20 ± 1.09	25.92 ± 2.35

Table 15: Sensitivity of original DD to a change in architecture (trained with AlexNet). The same order of examples used as during training, with the optimized learning rates. We have not been able to easily integrate ResNet-18 to the implementation provided by the authors (Wang et al. 2018).

	RR model	Standard model
MNIST	88.25 ± 0.37	87.07 ± 0.64
CIFAR-10	38.40 ± 0.41	37.16 ± 0.59
CIFAR-100	10.96 ± 1.08	8.93 ± 0.27
E → M	80.09 ± 1.84	76.04 ± 2.29
E → K	58.14 ± 0.91	50.37 ± 2.75
B → C	34.81 ± 6.46	35.76 ± 0.54
E → K-49	17.56 ± 1.62	13.28 ± 1.62

Table 16: Transferability of RR synthetic labels to standard model training (both within-dataset and cross-dataset scenarios evaluated). 100 base examples used. Datasets: E = EMNIST, M = MNIST, K = KMNIST, B = CUB, C = CIFAR-10, K-49 = Kuzushiji-49.

Base examples	10	20	50	100
MNIST (DD)	55.48 ± 4.42	17.90 ± 4.54	34.40 ± 4.49	34.44 ± 6.15
MNIST (DD RR)	22.33 ± 2.75	49.30 ± 2.72	30.16 ± 5.32	36.43 ± 5.50
CIFAR-10 (DD)	12.99 ± 1.41	12.09 ± 0.99	16.01 ± 1.48	17.92 ± 1.71
CIFAR-10 (DD RR)	20.20 ± 0.38	22.71 ± 0.79	26.04 ± 1.22	27.05 ± 1.86

Table 17: Dataset distillation of images. The results show we have not obtained strong and stable results when distilling synthetic images rather than labels (likely because of the complexity of the flexible task). It may be possible to obtain better results on distilling images with our approach, but it likely requires a lot more tuning than we have done.

	Second-order	RR
3	[0.00, 0.00, 0.01, 0.99, 0.00, 0.01, 0.00, 0.00, 0.00, 0.00]	[0.00, 0.01, 0.01, 0.76, 0.00, 0.00, 0.00, 0.20, 0.01, 0.00]
5	[0.00, 0.00, 0.00, 0.00, 0.00, 0.99, 0.00, 0.00, 0.00, 0.01]	[0.05, 0.01, 0.02, 0.06, 0.06, 0.38, 0.04, 0.00, 0.15, 0.23]
2	[0.00, 0.00, 0.99, 0.01, 0.00, 0.00, 0.00, 0.00, 0.00, 0.00]	[0.19, 0.00, 0.36, 0.28, 0.00, 0.00, 0.02, 0.00, 0.08, 0.08]
9	[0.00, 0.00, 0.00, 0.00, 0.02, 0.00, 0.00, 0.02, 0.00, 0.95]	[0.00, 0.00, 0.00, 0.00, 0.36, 0.00, 0.00, 0.32, 0.06, 0.26]
1	[0.00, 0.93, 0.00, 0.00, 0.00, 0.00, 0.00, 0.07, 0.00, 0.00]	[0.00, 0.73, 0.00, 0.05, 0.02, 0.00, 0.01, 0.07, 0.04, 0.09]
0	[0.99, 0.00, 0.00, 0.00, 0.00, 0.01, 0.00, 0.00, 0.00, 0.00]	[0.90, 0.00, 0.01, 0.01, 0.00, 0.07, 0.00, 0.00, 0.01, 0.00]
4	[0.00, 0.00, 0.00, 0.00, 0.99, 0.00, 0.00, 0.00, 0.00, 0.01]	[0.00, 0.00, 0.00, 0.03, 0.74, 0.04, 0.06, 0.00, 0.00, 0.12]
8	[0.00, 0.00, 0.02, 0.00, 0.00, 0.00, 0.00, 0.97, 0.00, 0.00]	[0.00, 0.00, 0.13, 0.01, 0.01, 0.14, 0.17, 0.00, 0.54, 0.00]
6	[0.00, 0.00, 0.00, 0.00, 0.00, 0.00, 1.00, 0.00, 0.00, 0.00]	[0.02, 0.01, 0.16, 0.00, 0.02, 0.00, 0.79, 0.00, 0.00, 0.00]
7	[0.00, 0.00, 0.00, 0.00, 0.00, 0.00, 0.00, 0.99, 0.00, 0.00]	[0.19, 0.07, 0.00, 0.00, 0.00, 0.05, 0.06, 0.56, 0.00, 0.06]
P	[0.35, 0.00, 0.02, 0.02, 0.03, 0.01, 0.00, 0.18, 0.04, 0.34]	[0.26, 0.00, 0.01, 0.09, 0.04, 0.00, 0.02, 0.19, 0.12, 0.27]
w	[0.00, 0.42, 0.03, 0.01, 0.14, 0.01, 0.31, 0.00, 0.06, 0.03]	[0.00, 0.23, 0.10, 0.00, 0.19, 0.02, 0.20, 0.01, 0.12, 0.13]
h	[0.00, 0.00, 0.08, 0.01, 0.00, 0.01, 0.00, 0.79, 0.00, 0.11]	[0.01, 0.00, 0.07, 0.08, 0.00, 0.01, 0.29, 0.49, 0.00, 0.05]
x	[0.00, 0.00, 0.00, 0.00, 0.00, 0.00, 0.00, 0.02, 0.01, 0.97]	[0.06, 0.13, 0.22, 0.00, 0.03, 0.00, 0.00, 0.04, 0.19, 0.32]
F	[0.00, 0.01, 0.17, 0.29, 0.21, 0.01, 0.14, 0.16, 0.00, 0.01]	[0.00, 0.11, 0.16, 0.16, 0.11, 0.00, 0.21, 0.22, 0.00, 0.04]
K	[0.00, 0.02, 0.00, 0.01, 0.00, 0.01, 0.00, 0.02, 0.86, 0.08]	[0.00, 0.36, 0.00, 0.32, 0.00, 0.00, 0.05, 0.00, 0.22, 0.04]
C	[0.00, 0.00, 0.00, 0.49, 0.00, 0.28, 0.00, 0.24, 0.00, 0.00]	[0.05, 0.03, 0.01, 0.10, 0.03, 0.20, 0.00, 0.57, 0.01, 0.00]
J	[0.45, 0.03, 0.05, 0.05, 0.05, 0.10, 0.03, 0.11, 0.06, 0.08]	[0.16, 0.06, 0.01, 0.07, 0.05, 0.33, 0.08, 0.10, 0.01, 0.14]
J	[0.11, 0.00, 0.00, 0.03, 0.03, 0.73, 0.00, 0.08, 0.01, 0.01]	[0.17, 0.02, 0.11, 0.26, 0.10, 0.24, 0.08, 0.01, 0.00, 0.01]
r	[0.00, 0.00, 0.57, 0.01, 0.00, 0.05, 0.05, 0.05, 0.21, 0.10]	[0.01, 0.00, 0.30, 0.03, 0.00, 0.19, 0.15, 0.23, 0.06, 0.03]

Figure 6: Examples of distilled labels for both second-order and RR label distillation. The upper part shows base examples and their distilled labels for within-dataset MNIST scenario with 10 base examples. The lower part shows EMNIST (“English”) base examples and their synthetic labels that allow the model to learn to classify KMNIST (“Japanese”) characters – 10 base examples used.

	Second-order	RR
	[0.03, 0.47, 0.04, 0.03, 0.03, 0.04, 0.03, 0.02, 0.11, 0.21]	[0.00, 0.48, 0.07, 0.01, 0.02, 0.11, 0.00, 0.01, 0.14, 0.17]
	[0.13, 0.21, 0.01, 0.01, 0.01, 0.00, 0.00, 0.03, 0.15, 0.46]	[0.22, 0.14, 0.05, 0.03, 0.01, 0.00, 0.00, 0.05, 0.14, 0.35]
	[0.00, 0.01, 0.31, 0.00, 0.29, 0.01, 0.34, 0.03, 0.00, 0.01]	[0.00, 0.04, 0.25, 0.05, 0.19, 0.03, 0.38, 0.06, 0.01, 0.00]
	[0.61, 0.02, 0.04, 0.00, 0.01, 0.00, 0.00, 0.00, 0.32, 0.00]	[0.42, 0.09, 0.10, 0.01, 0.01, 0.00, 0.00, 0.00, 0.35, 0.02]
	[0.03, 0.01, 0.25, 0.07, 0.24, 0.15, 0.10, 0.14, 0.00, 0.01]	[0.00, 0.02, 0.15, 0.08, 0.10, 0.18, 0.16, 0.27, 0.00, 0.03]
	[0.01, 0.05, 0.02, 0.27, 0.07, 0.35, 0.10, 0.08, 0.02, 0.03]	[0.03, 0.01, 0.08, 0.25, 0.12, 0.31, 0.02, 0.16, 0.02, 0.00]
	[0.28, 0.04, 0.04, 0.00, 0.02, 0.00, 0.00, 0.00, 0.53, 0.09]	[0.32, 0.00, 0.00, 0.00, 0.07, 0.00, 0.00, 0.06, 0.52, 0.03]
	[0.01, 0.07, 0.04, 0.22, 0.02, 0.16, 0.11, 0.14, 0.03, 0.19]	[0.01, 0.07, 0.04, 0.17, 0.02, 0.10, 0.13, 0.17, 0.04, 0.26]
	[0.05, 0.08, 0.11, 0.14, 0.15, 0.15, 0.19, 0.11, 0.00, 0.03]	[0.08, 0.03, 0.16, 0.11, 0.22, 0.10, 0.21, 0.00, 0.07, 0.01]
	[0.03, 0.01, 0.17, 0.08, 0.27, 0.10, 0.15, 0.18, 0.00, 0.01]	[0.00, 0.01, 0.14, 0.13, 0.27, 0.06, 0.24, 0.16, 0.00, 0.00]
	[0.04, 0.37, 0.01, 0.04, 0.01, 0.05, 0.07, 0.03, 0.11, 0.28]	[0.03, 0.15, 0.04, 0.11, 0.04, 0.11, 0.11, 0.05, 0.16, 0.20]
	[0.01, 0.00, 0.24, 0.06, 0.32, 0.08, 0.13, 0.15, 0.00, 0.00]	[0.04, 0.03, 0.16, 0.10, 0.23, 0.07, 0.11, 0.22, 0.02, 0.02]
	[0.18, 0.12, 0.08, 0.08, 0.06, 0.07, 0.03, 0.06, 0.17, 0.14]	[0.20, 0.06, 0.12, 0.12, 0.06, 0.09, 0.05, 0.07, 0.13, 0.10]
	[0.00, 0.02, 0.13, 0.18, 0.13, 0.17, 0.18, 0.18, 0.00, 0.01]	[0.02, 0.04, 0.18, 0.14, 0.10, 0.13, 0.19, 0.18, 0.00, 0.02]
	[0.00, 0.01, 0.06, 0.09, 0.04, 0.20, 0.06, 0.52, 0.00, 0.01]	[0.06, 0.10, 0.12, 0.10, 0.09, 0.12, 0.05, 0.26, 0.00, 0.10]
	[0.53, 0.02, 0.03, 0.00, 0.01, 0.00, 0.00, 0.01, 0.35, 0.03]	[0.32, 0.09, 0.04, 0.00, 0.03, 0.00, 0.00, 0.00, 0.44, 0.09]
	[0.02, 0.06, 0.09, 0.22, 0.18, 0.19, 0.17, 0.06, 0.00, 0.01]	[0.05, 0.09, 0.04, 0.10, 0.21, 0.18, 0.17, 0.11, 0.05, 0.00]
	[0.00, 0.00, 0.35, 0.00, 0.29, 0.00, 0.09, 0.25, 0.00, 0.00]	[0.02, 0.03, 0.16, 0.02, 0.24, 0.00, 0.31, 0.07, 0.02, 0.11]
	[0.04, 0.02, 0.16, 0.17, 0.15, 0.19, 0.17, 0.09, 0.00, 0.01]	[0.00, 0.01, 0.21, 0.09, 0.20, 0.16, 0.10, 0.15, 0.04, 0.03]
	[0.01, 0.00, 0.23, 0.02, 0.31, 0.04, 0.33, 0.05, 0.00, 0.00]	[0.03, 0.02, 0.21, 0.10, 0.17, 0.07, 0.38, 0.02, 0.00, 0.00]

Figure 7: Examples of distilled labels for both second-order and RR label distillation. The upper part shows base examples and their distilled labels for within-dataset CIFAR-10 scenario with 10 base examples. The lower part shows CUB (birds) base examples and their synthetic labels that allow the model to learn to classify CIFAR-10 objects – 10 base examples used.

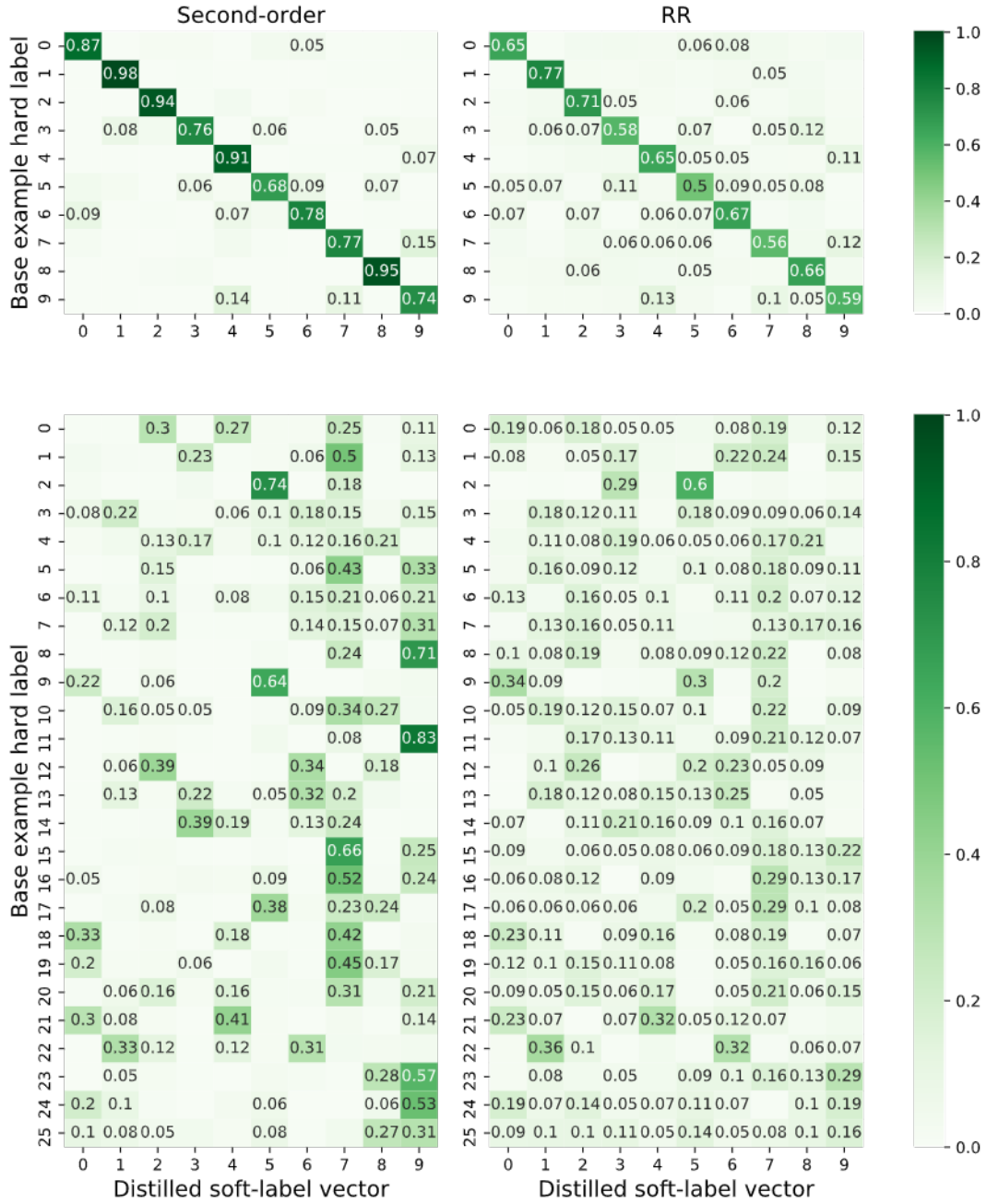


Figure 8: Distribution of label values across base example hard labels and distilled soft-label vectors. The upper row shows the mean distilled labels for different original classes for within-dataset MNIST scenario with 100 base examples. We can see that to a large extent the original labels are preserved with an additional noise on visually similar classes such as 4 and 9. At the same time, some non-trivial information is learned, especially for our RR method. The lower row shows the mean distilled labels for different original EMNIST (“English”) classes used to recognize KMNIST (“Japanese”) characters. 100 base examples scenario. Numbers are shown when the values are at least 0.05.

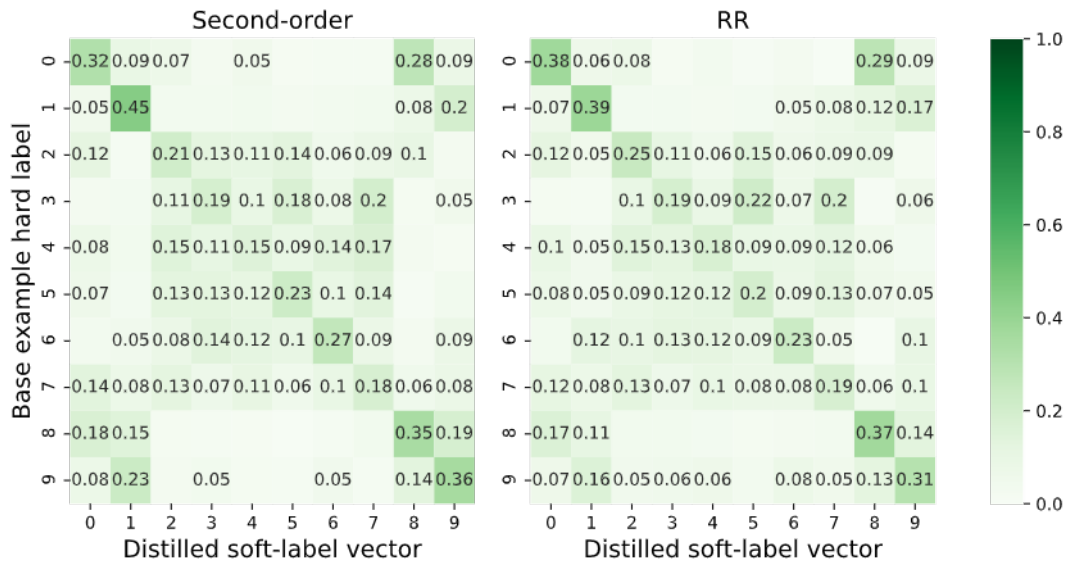


Figure 9: Distribution of label values across base example hard labels and distilled soft-label vectors. Within-dataset CIFAR-10 scenario with 100 base examples is shown. We can see that to a certain extent the original classes are recovered, but a lot of non-trivial information is added that presumably leads to strong improvements over a baseline with true or smooth labels. Numbers are shown when the values are at least 0.05.

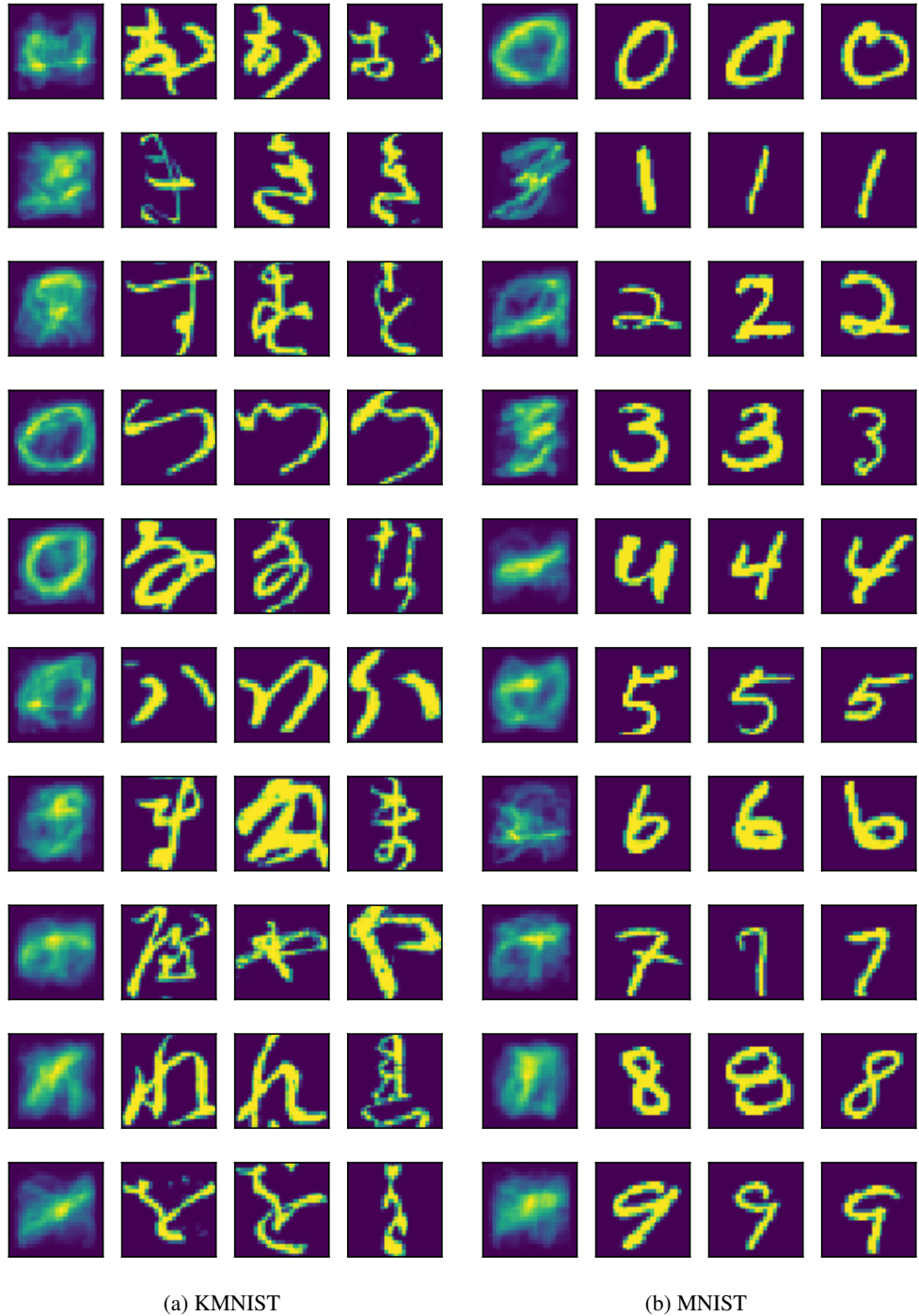


Figure 10: Cross-dataset task: reconstructed images from KMNIST (Japanese letters) and MNIST (digits) based on combination of EMNIST base examples (English letters). 100 base examples used in both cases. Each row corresponds to a separate class, while the leftmost column shows the reconstructed image and the other three columns show actual examples from the same class. One image is reconstructed for each target dataset class. The base example images are combined pixel-wise with proportions based on the element of the synthetic label vector corresponding to the class that is being reconstructed. Note that KMNIST images in the same class can look very different because of different ways of writing the character, which makes reconstruction more challenging. Some of the reconstructed images resemble images from the target dataset classes, which suggests LD learns labels that combine base examples so that their pixel-wise combination, weighted based on the synthetic class labels, looks similar to images from the target dataset.